Optical simulation and experimental verification of single slit diffraction and circular hole diffraction

Yuhao Li* and Yifeng Deng†
School of Physics, Sun Yat-sen University, Guangzhou, Guangdong, China
(Dated: November 15, 2022)

Fronhofer diffraction of a single slit, Fresnel diffraction and Fronhofer diffraction of a circular hole, are three basic types of diffraction. We first deduce the results of the these diffractions theoretically and verify them experimentally. Using simulations, we further study the diffraction patterns and observe the triple splitting of the primary maximum in the Frontier diffraction pattern of the laser.

I. INTRODUCTION

Diffraction of light is one of the basic characteristics of light fluctuation, which is widely used in spectral analysis, crystal analysis, holography, light information processing and other precision measurement and modern optical technology. Diffraction of light refers to the phenomenon that when light encounters an obstacle or a small aperture in the process of propagation, the light will deviate from the path of linear propagation and propagate around behind the obstacle. According to the distance between light source and aperture, aperture and observation screen, diffraction can be divided into Fresnel diffraction and Fronhofer diffraction; according to the type of obstacle, diffraction can be divided into single-slit diffraction, multi-slit diffraction, circular aperture diffraction, etc.. Among them, the more basic ones are single-slit Fronhofer diffraction, circular-hole Fresnel diffraction, and Fronhofer diffraction. Studying the basic principles and physical images of these three diffractions clearly is essential for understanding the diffraction of light and for further optical learning and research.

Fresnel was the first physicist to theoretically solve the distribution of diffracted fields, and in 1818 he successfully explained the diffraction phenomenon by introducing the concept of "coherent superposition of subwaves", based on the concept of subwaves in Huygens' principle and the idea of light wave interference. In 1880, Kirchhoff derived the expression for the edge-valued definite boundary of the passive space by using the Green's formula of vector field theory. In contrast to the Fresnel diffraction integral, Kirchhoff made an important contribution to the practical solution of diffraction fields by specifying the expressions for the tilt factor and the scale factor, and by pointing out that the integration surface is not limited to the isophase surface.

Kirchhoff made some assumptions about the boundary conditions, called Kirchhoff boundary conditions, in order to change the integration surface of the Fresnel diffraction integral formula into a finite surface. However, from the viewpoint of the strict electromagnetic wave theory, Kirchhoff's boundary conditions are not self-consistent, and its treatment of the light field does not satisfy the boundary conditions of the electromagnetic field. The strict diffraction theory of light waves should be based on the vector wave diffraction theory of high-frequency electromagnetic fields, whose boundary conditions are significantly different from the Kirchhoff boundary conditions. However, in general, the diffraction field we solve for satisfies the condition of paraxiality and the condition that the long period of the optical wave is smaller than the linearity of the optical aperture, so some approximations can be made to the Kirchhoff diffraction integral equation to obtain the more commonly used paraxial diffraction integral equation.

According to the distance between the light source, diffraction screen and receiving screen, diffraction systems can be divided into two categories: Fresnel diffraction and Fronhofer diffraction. The diffraction system is Fresnel diffraction, or near-field diffraction, when at least one of the distances between the source-diffraction screen and the diffraction screen-receiving screen is finite; when both distances are infinite, the diffraction system is Fronhofer diffraction, or far-field diffraction. From the theoretical point of view, Fronhofer diffraction is a special case of Fresnel diffraction, but from the practical point of view, the theoretical calculation and experimental implementation of Fronhofer diffraction are easier and more valuable for application, and it is closely related to Fourier optics in modern transformation optics.

In this paper, we first give a formula for the Fronhofer diffraction of a single slit based on the integral formula for paraxial diffraction, and then discuss the Fresnel diffraction of a circular hole using the half-wave band theory and give a detailed derivation of the formula for the Fronhofer diffraction of a circular hole. We have verified these theories experimentally and made further investigations using simulations. We observed the triple splitting of the primary maximum in the Fronhofer diffraction pattern of the laser and found some related theoretical explanations by reviewing other literature.

* liyh536@mail2.sysu.edu.cn; student number:21305412
† Experimental collaborator

II. THEORY OF DIFFRACTION

A. Diffraction theory of scalar light waves

Huygens proposed a hypothesis in 1690: each point on the wavefront can be considered as a secondary perturbation center emitting a spherical subwave, and the envelope of these subwaves at a later time is the new wavefront at that time.

Fresnel added to the Huygens principle based on the interference theory of light: considering that the Huygens subwaves come from the same source, they should be coherent, and thus the optical vibration at any point outside the wavefront should be the result of a coherent superposition of all the subwaves on the wavefront at that point. the mathematical expression of the Huygens-Fresnel principle is written as

$$\widetilde{E}(P) = C \iint_{\Sigma} \widetilde{E}(Q) \frac{\exp(\mathrm{i}kr)}{r} K(\theta) \mathrm{d}\sigma \qquad (1)$$

where C is the constant of proportionality, $\widetilde{E}(Q)$ is the complex amplitude distribution of the sub-wave source itself, $\frac{\exp(\mathrm{i}kr)}{r}$ is the perturbation of the sub-waves emitted by the surface element on the sub-wave source at the field point, and $K(\theta)$ is the tilt factor.

Kirchhoff's work in fact complements the scaling constant and tilt factor in Eq. (1)

$$C = \frac{1}{\mathrm{i}\lambda} \qquad K(\theta) = \frac{\cos(n,r) - \cos(n,l)}{2} \qquad (2)$$

where λ is the wavelength of light, which also indicates that the equation applies only to monochromatic waves.i is the imaginary unit, which indicates that the vibrational phase of the subwave source is 90° ahead of the incident wave.(n,r) and (n,l) indicate the angle between the two lines, see Fig.1 for the specific meaning.

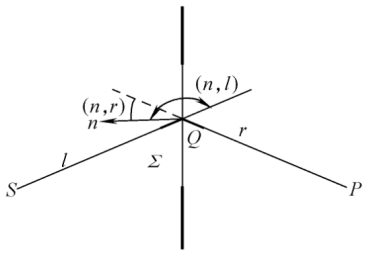

FIG. 1. Explanation of each physical quantity in the expression of diffraction integral

The paraxial approximation means that the monochromatic wave is incident vertically on the aperture Σ, which requires that $(n,r),(n,l) < 0.5$ rad.And both the linearity of the diffracted aperture and the linearity of the diffraction pattern on the viewing screen are much smaller than the distance from the aperture to the viewing screen.Therefore we can make the following approximation

$$K(\theta) = \frac{\cos(n,r) - \cos(n,l)}{2} \approx 1, \frac{\exp(\mathrm{i}kr)}{r} \approx \frac{1}{z}\exp(\mathrm{i}kr)$$

where the effect of the variation of r in the complex index on the phase cannot be neglected and cannot be approximated as the distance z from the hole to the observation screen. The integral equation for the paraxial diffraction can be written as

$$\widetilde{E}(P) = \frac{1}{\mathrm{i}\lambda z} \iint_{\Sigma} \widetilde{E}(Q) \exp(\mathrm{i}kr) \mathrm{d}\sigma \qquad (3)$$

Next, we have a further discussion of r in the right-angle coordinate system in space.Taking the right angle coordinates of the plane where the diffraction screen is located as (x1, y1) and the right angle coordinates of the plane where the receiving screen is located as (x, y), then r can be expressed as

$$r = \sqrt{z^2 + (x - x_1)^2 + (y - y_1)^2}$$

Performing a Taylor expansion on r and taking only the first two terms, when the condition $\frac{k}{8z^3}\left[(x-x_1)^2 + (y-y_1)^2\right]^2_{\max} << \pi$ (called Fresnel approximation) is satisfied:

$$r \approx z + \frac{x^2+y^2}{2z} - \frac{xx_1 + yy_1}{z} + \frac{x_1^2 + y_1^2}{2z} \qquad (4)$$

The fourth term in the above equation all decreases as z increases. The fourth term can be ignored when z is large enough to satisfy the condition $k\frac{(x_1^2+y_1^2)_{\max}}{2z} << \pi$(called the Fronhofer approximation). Under this approximation r can be written as

$$r \approx z + \frac{x^2+y^2}{2z} - \frac{xx_1 + yy_1}{z} \qquad (5)$$

Substituting it into Eq. (3), we get the Fronhofer diffraction integral formula, which is the basis for the quantitative solution of the diffraction field in the next subsection.

$$\widetilde{E}(P) = \frac{1}{\mathrm{i}\lambda z}\exp(\mathrm{i}kz)\exp\left[\frac{\mathrm{i}k}{2z}(x^2+y^2)\right] \iint_{\Sigma} \widetilde{E}(Q)\exp\left[-\frac{\mathrm{i}k}{z}(xx_1+yy_1)\right]\mathrm{d}\sigma \qquad (6)$$

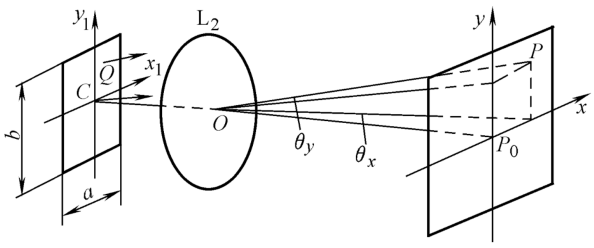

FIG. 2. Fronhofer diffraction of a rectangular hole

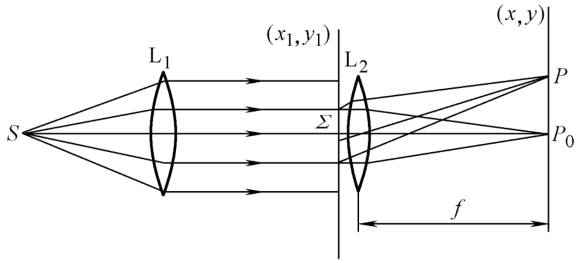

FIG. 3. Schematic diagram of Fronhofer diffraction device

B. Fraunhofer diffraction of a single slit

The Fraunhofer diffraction of a single slit is actually a generalization of the Fraunhofer diffraction of a rectangular hole.We first consider the Fronhofer diffraction of a rectangular hole as shown in Fig.2.

Since Fronhofer diffraction requires the distance from the light source to the diffraction screen and from the diffraction screen to the observation screen to be infinite. Usually, as shown in Fig.3, a convex lens is placed in front of the diffraction screen to change the light from the point source into parallel light, and a convex lens is placed behind the diffraction screen to converge the diffraction pattern observed at infinity to the focal plane of the lens.

When the lens is close to the diffraction screen, the center of the lens can be considered to coincide with the coordinate origin of the diffraction screen.r can be written as

$$r \approx f + \frac{x^2+y^2}{2f}$$

And then Eq. (6) can be rewritten as

$$\begin{aligned}\widetilde{E} &= C' \exp\left[\mathrm{i}k\left(\frac{x^2+y^2}{2f}\right)\right] \int_{-\frac{a}{2}}^{\frac{a}{2}} \exp\left(-\mathrm{i}k\sin\theta_x x_1\right) \mathrm{d}x_1 \int_{-\frac{b}{2}}^{\frac{b}{2}} \exp\left(-\mathrm{i}k\sin\theta_y y_1\right) \mathrm{d}y_1 \\ &= \widetilde{E}_0 \left(\frac{\sin\frac{\sin\theta_x a}{2}}{\frac{k\sin\theta_x a}{2}}\right)\left(\frac{k\sin\theta_y b}{\frac{k\sin\theta_y b}{2}}\right) \exp\left[\mathrm{i}k\left(\frac{x^2+y^2}{2f}\right)\right]\end{aligned} \tag{7}$$

where $C' = \frac{CA'}{f}\exp(\mathrm{i}kf)$, A' means that the complex amplitude $\widetilde{E}(Q)$ is a constant A' when the plane wave is incident vertically on the diffraction screen. The light intensity distribution is

$$\begin{aligned}I = |\widetilde{E}|^2 &= I_0 \left(\frac{\sin\frac{k\sin\theta_x a}{2}}{\frac{k\sin\theta_x a}{2}}\right)^2 \left(\frac{k\sin\theta_y b}{\sin\frac{k\sin\theta_y b}{2}}\right)^2 \\ &= I_0 \left(\frac{\sin\alpha}{\alpha}\right)^2 \left(\frac{\sin\beta}{\beta}\right)^2\end{aligned} \tag{8}$$

where I_0 is the light intensity at point P_0, and α, β is

$$\alpha = \frac{k\sin\theta_x a}{2} = \frac{\pi}{\lambda} a\sin\theta_x,\ \beta = \frac{k\sin\theta_y b}{2} = \frac{\pi}{\lambda} b\sin\theta_y$$

A single slit is actually a rectangular hole with one side much smaller in width than the other, e.g. $b \gg a$, so the diffraction effect of the incident light in the y-axis direction can be neglected and the diffraction pattern is distributed only on the x-axis. The light intensity distribution of single-slit diffraction is

$$I = I_0 \left(\frac{\sin\alpha}{\alpha}\right)^2 \tag{9}$$

The relative light intensity distribution of the single-slit Fraunhofer diffraction pattern plotted according to Eq. (9) is shown in Fig.4

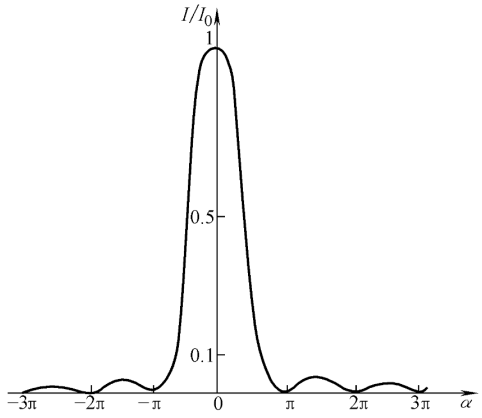

FIG. 4. The relative light intensity distribution of the single-slit Fraunhofer diffraction pattern

C. Fresnel diffraction of a circular hole

We make the Fresnel approximation and the Fronhofer approximation for r in Section II A. Substituting the Fresnel approximation Eq. (4) for r into the integral equation for the paraxial diffraction, the diffracted field can be solved quantitatively as in Section II B. However, we can also obtain the diffraction pattern and spatial light field distribution by another semi-quantitative method, called the half-waveband method.

Suppose a monochromatic plane wave is incident perpendicular to the circular aperture and the wavefront within the aperture is Σ. Now a series of spherical surfaces are made with P_0 as the center and $z_1 + \frac{\lambda}{2}, z_1 + \lambda, \cdots, z_1 + \frac{j\lambda}{2}, \cdots$ as the radius. These spherical surfaces intersect with Σ to form a circle, and Σ is divided into a ring of bands [see Fig.5], which are called Fresnel half-wave bands. According to the Huygens-Fresnel principle, the complex amplitude at the point P_0 is the superposition of the complex amplitudes of the subwaves emitted by all the bands on the wavefront Σ at the point P_0. The amplitude of each band at P_0 is proportional to the area of the band, and inversely proportional to the distance from the band to P_0, and depends on the tilt factor K. Let the band at the center of the circle C be the first band, and the outward bands 2, 3, ... j, ... Then the amplitude of the jth band at P_0 can be expressed as

$$\left|\widetilde{E}_j\right| = C\frac{A_j 1+\cos\theta}{r_j} \tag{10}$$

where C is a constant of proportionality, r_j is the distance of the j waveband to point P_0, and A_j is the area of the j waveband. When $z_1 \gg \lambda$, there is

$$\rho_j = \left[\left(z_1 + j\frac{\lambda}{2}\right)^2 - z_1^2\right]^{1/2} \approx \sqrt{jz_1\lambda}$$

thus

$$A_j \approx \pi\rho_j^2 - \pi\rho_{j-1}^2 \approx \pi z_1\lambda$$

which shows that the areas of the individual bands are approximately equal.The amplitude generated by each waveband at point P_0 is only related to the distance and inclination factor of each waveband to point P_0. The larger the number j of the waveband, the larger the distance r_j and the tilt angle, so that the amplitude of the vibration of each waveband at point P_0 will decrease monotonically with the increase of j.

Considering that the optical range difference of adjacent bands to P_0 is half a wavelength, the phase difference of their subwaves to P_0 is π. So the complex amplitudes of adjacent bands are one positive and one negative, the total complex amplitude of each band at P_0 is

$$\widetilde{E} = \left|\widetilde{E}_1\right| - \left|\widetilde{E}_2\right| + \left|\widetilde{E}_3\right| - \left|\widetilde{E}_4\right| + \cdots - (-1)^n\left|\widetilde{E}_n\right| \tag{11}$$

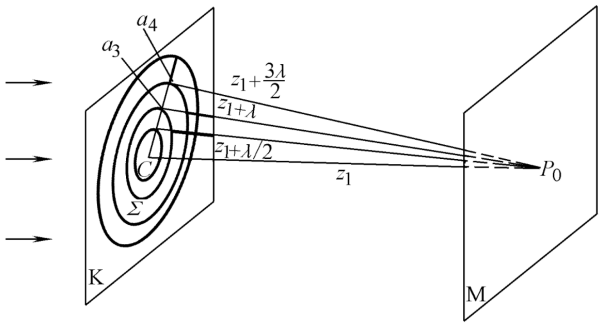

FIG. 5. Half-waveband method for splitting wavefront

When the number of wavebands n is large enough, the difference between $|E_{n-1}|$ and $|E_n|$ is small, so that Eq. (11) can be written as

$$\widetilde{E} = \frac{\left|\widetilde{E}_1\right|}{2} \pm \frac{\left|\widetilde{E}_n\right|}{2} \tag{12}$$

In the above equation, the sign "+" is taken when n is odd, and the sign "-" is taken when n is even. This means that the center of the diffraction pattern changes in light and dark along with the odd-even variation of the number of half-wave bands. This is the periodic variation of the diffraction field along the longitudinal direction.

D. Fronhofer diffraction of a circular hole

The Fronhofer diffraction of a circular hole is still calculated based on the Fronhofer diffraction integral formula Eq.(6). However, since the integration interval is a circular surface and the calculation is very complicated, most of the optics textbooks only give the final light intensity distribution formula instead of discussing it in detail. In this subsection, we refer to the textbook [1] to give the solution procedure.

We need to rewrite Eq.(6) in the polar coordinate system.Considering the conversion relationship between right-angle coordinate system and polar coordinate system

$$\begin{aligned} &x_1 = r_1\cos\psi_1 \quad y_1 = r_1\sin\psi_1 \\ &x = r\cos\psi \quad y = r\sin\psi \\ &\mathrm{d}\sigma = r_1\ \mathrm{d}r_1\ \mathrm{d}\psi_1 \end{aligned}$$

so

$$\frac{x}{f} = \frac{r\cos\psi}{f} = \theta\cos\psi \quad \frac{y}{f} = \frac{r\sin\psi}{f} = \theta\sin\psi$$

where θ is the diffraction angle (the angle between the diffraction direction OP and the optical axis).

Substituting the above relationship into the Eq. (6) we can get the complex amplitudes at point P

$$\begin{aligned}\widetilde{E}(P) &= C' \int_0^a \int_0^{2\pi} \exp\left[-ik\left(r_1\theta\cos\psi_1\cos\psi + r_1\theta\sin\psi_1\sin\psi\right) r_1 \ \mathrm{d}r_1 \ \mathrm{d}\psi_1\right] \\ &= C' \int_0^a \int_0^{2\pi} \exp\left[-\mathrm{i}kr_1\theta\cos\left(\psi_1-\psi\right) r_1 \ \mathrm{d}r_1 \ \mathrm{d}\psi_1\right]\end{aligned} \tag{13}$$

where $C' = \frac{CA}{f}\exp(ikf)$; the other phase factor $\exp\left[ik\left(\frac{x^2+y^2}{2f}\right)\right]$ is eliminated in the calculation of the light intensity and has been omitted in the above equation for simplicity.

According to the integral representation of the Bessel function of order zero and the recurrence relation of the Bessel function

$$\begin{aligned}&\frac{1}{2\pi}\int_0^{2\pi}\exp\left(-\mathrm{i}kr_1\theta\cos\psi_1\right)\mathrm{d}\psi_1 = \mathrm{J}_0\left(kr_1\theta\right) \\ &\frac{\mathrm{d}}{\mathrm{d}z}\left[Z\ \mathrm{J}_1(Z)\right] = Z\ \mathrm{J}_0(Z)\end{aligned} \tag{14}$$

Eq.(13) can be rewritten as

$$\begin{aligned}\widetilde{E}(P) &= 2\pi C' \int_0^a \mathrm{J}_0\left(kr_1\theta\right) r_1 \ \mathrm{d}r_1 \\ &= \frac{2\pi C'}{(k\theta)^2}\int_0^{ka\theta}\left(kr_1\theta\right)\mathrm{J}_0\left(kr_1\theta\right)\mathrm{d}\left(kr_1\theta\right) \\ &= \pi a^2 C' \frac{2\ \mathrm{J}_1(ka\theta)}{ka\theta}\end{aligned}$$

so the light intensity at point P is

$$I = \left(\pi a^2\right)^2 |C'|^2 \left[\frac{2\ \mathrm{J}_1(ka\theta)}{ka\theta}\right]^2 = I_0\left[\frac{2\ \mathrm{J}_1(Z)}{Z}\right]^2 \tag{15}$$

where $I_0 = \left(\pi a^2\right)^2 |C'|^2$ is the light intensity at point P_0, and $Z = ka\theta$.Based on Eq.(15), the relative light intensity distribution of the Fronhofer diffraction of a circular hole can be plotted as shown in Fig.6.

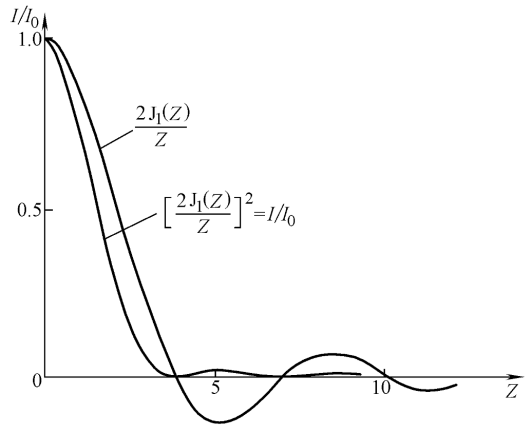

FIG. 6. The relative light intensity distribution of the Fronhofer diffraction of a circular hole

It can be seen that the intensity of the submaximum is much less than that of the central primary maximum. In the diffraction pattern, the majority of the light energy is concentrated in the central bright spot, commonly called the Airy spot. The radius r_0 of the Airy spot is determined by the value of Z corresponding to the first intensity of zero.

$$Z = \frac{kar_0}{f} = 1.22\pi$$

So

$$r_0 = 1.22f\frac{\lambda}{2a}, \quad \theta_0 = \frac{r_0}{f} = \frac{0.61\lambda}{a} \tag{16}$$

This indicates that the size of the diffraction spot is inversely proportional to the radius of the circular aperture and directly proportional to the wavelength of the light wave.

III. EXPERIMENT

We have done experiments on single slit Fronhofer diffraction, circular hole Fresnel diffraction and circular hole Fronhofer diffraction to verify the conclusions of subsection B.C&D in Section.II respectively.

A. Fraunhofer diffraction of a single slit

We have performed a single-slit Fraunhofer diffraction experiment using a laser. Unlike the theoretical derivation in the previous section, the laser can be regarded as a parallel source when directly incident on the slit due to its small divergence angle. Moreover, when the distance between the observation screen and the slit is far enough, we can consider him as infinity, which requires the following conditions to be satisfied:

$$\frac{a^2}{8Z\lambda} \ll 1 \tag{17}$$

This equation ensures that the maximum optical range difference between the secondary waves emitted from each point on the slit arriving at point P_0 is much smaller than the wavelength *lambda*.

We used a He-Ne laser with a wavelength of 632.8 nm, a slit width of 0.25 mm, and a distance from the observation screen to the slit of 1.07 m. We measured the light intensity distribution of the diffraction pattern in the x-axis direction and compared it with the theoretical value, as shown in Fig.7(a).

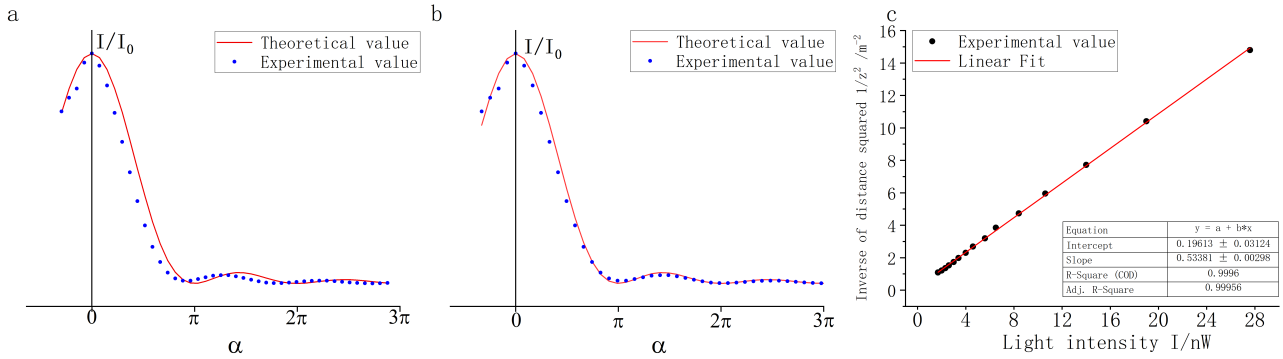

FIG. 7. (a) Relative light intensity distribution of single slit Fraunhofer diffraction. (b) Relative light intensity distribution after fixing the system deviation. (c) Calibration of the linear working interval of the optical power meter.

It is noted that there is a systematic deviation between the relative light intensity distribution obtained from our experiments and the theoretical value. We believe that this may be caused by errors in the measurement of the slit width, since the instrument we used to measure the slit width was not calibrated. So we tried to adjust the slit width used in the theoretical calculation and set it to 0.27 mm when the result is shown in Fig.7(b). It can be seen that the experiment and the theory are in good agreement.

In addition, we have calibrated the optical power meter using a bromine tungsten lamp. As shown in Fig.7(c), the linearity of the optical power meter is good in the interval we used.

B. Fresnel diffraction of a circular hole

In the Fresnel circular aperture diffraction experiment, we verified semi-quantitatively the correctness of the half-wave band theory. We observed that when the observation screen is moved in the longitudinal direction, the central spot appears to change brightly, which is in accordance with the theoretical prediction of the half-wave band. We recorded the locations of the bright and dark spots appearing at different apertures and compared them with the theoretical values, as shown in Table I.

Due to the space limitation of our experiment, we can only verify in the range of 10 cm to 1 m. The number of half-wave bands that can be observed varies for different radius of small holes. The larger the radius of the holes, the larger the number of half bands we can observe. In general, the locations where we observe the appearance of bright and dark spots are consistent with the half-wave band theory.

We took a photograph of the diffraction pattern and processed it using MATLAB to make the relative light intensity distribution in the x-axis direction, as shown in Fig.8. The diffraction pattern we obtained is not very beautiful due to the limited shooting equipment. However, it can still be seen that the center of the pattern is clearly a dark spot.

TABLE I. Verification of the longitudinal light intensity distribution of the Fresnel circular hole diffraction pattern. The focal length of the beam expander is 4.5 mm, the distance from the beam expander to the small hole is 20 cm, and the radius of the circular holes are 0.75 mm, 0.5 mm, and 0.35 mm, respectively.

$\rho = 0.75$ mm

j[a]	Center	Location/cm[b]	Theory/cm
6	dark	61.7	61.1
7	bright	38.4	36.2
8	dark	25.4	25.7
9	bright	20.7	19.9

$\rho = 0.5$ mm

j	Center	Location/cm	Theory/cm
3	bright	41.9	40.3
4	dark	21.8	19.9

$\rho = 0.35$ mm

j	Center	Location/cm	Theory/cm
2	dark	20.1	19.1
3	bright	9.5	9.6

[a] Number of half-wave bands
[b] Experimentally measured locations of bright and dark spots

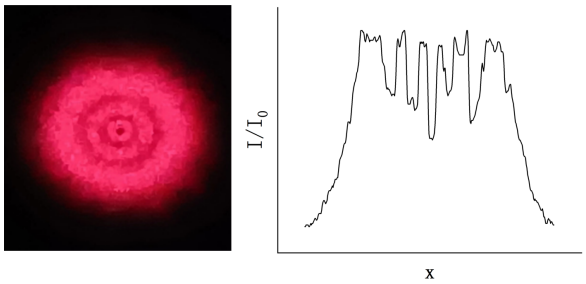

FIG. 8. The relative light intensity distribution of the Fresnel diffraction of a circular hole

C. Fronhofer diffraction of a circular hole

In the Fronhofer diffraction experiments of a circular hole, we mainly measured the diameter of the Airy spot produced by small holes of different radius. As in subsectionA, we used a laser to generate a parallel light source for Fronhofer diffraction. We used a He-Ne laser with a wavelength of 632.8 nm and set the distance from the viewing screen to the aperture as 1 m. The diameters of the Airy spots calculated using Eq.(16) and measured experimentally are shown in Table II.

TABLE II. The diameters of the Airy spots calculated using Eq.(16) and measured experimentally

Diameter/mm[a]	Theory/mm	Experiment/mm
0.15	10.29	9.8
0.3	5.15	6.3
0.5	3.09	3.4

[a] Diameter of the circular hole

As shown in Fig.9, as the diameter of the circular hole increases, the distance between the stripes becomes smaller, and there is greater human error in distinguishing the edge of the Airy spot and measuring its diameter.Therefore, here, we only do a rough verification of the Fronhofer diffraction. More detailed discussion and validation will be given in the simulation section.

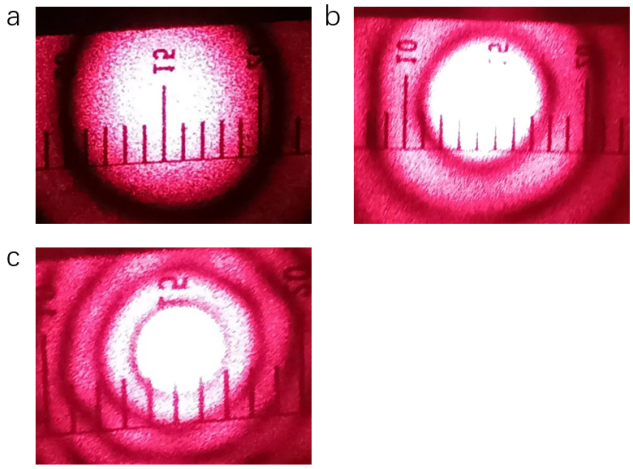

FIG. 9. Measurement of Airy spot diameter in the experiment. (a)$\phi = 0.15$ mm. (b)$\phi = 0.3$ mm. (c)$\phi = 0.5$ mm

In addition, we also took photographs of the Fronhofer diffraction pattern and made relative light intensity distribution curves, as shown in Fig.10. We took the photos with a slightly larger exposure, which has the advantage of seeing more submaximum bright lines, but the disadvantage of not showing the intensity distribution of the central bright lines.

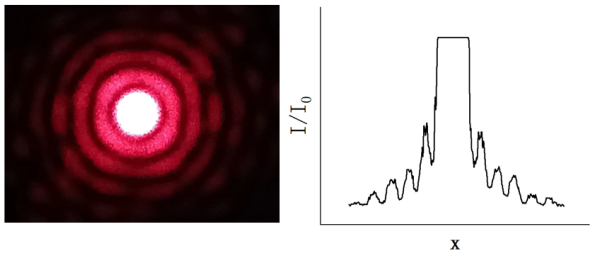

FIG. 10. The relative light intensity distribution of the Fronhofer diffraction of a circular hole

IV. SIMULATION

A. Fronhofer diffraction of slits with different widths

We simulated the Fronhofer diffraction from a single slit with the help of the seelight optical simulation platform and explored the effect of the slit width on the diffraction pattern.

The device diagram of Fronhofer diffraction with a single slit is shown in Fig.11 (a). We set the diameter of the light source as 1mm, the diameter of the circular hole as 0.2mm, 0.3mm, 0.4mm, 0.5mm, and the distance of vacuum transmission as 5m. The diffraction patterns of these four slits with different widths are shown in Fig.11 (c). We plot the relative light intensity distribution curves of the four diffraction patterns in the same figure, as shown in Fig.11 (b).

It can be seen that as the slit width increases, the width of the central bright spot is decreasing and the brightness is increasing; the distance between the individual stripes is decreasing. This is in accordance with our derivation in Section II B. From another point of view, it is also consistent with our physical intuition. Diffraction occurs when the size of the barrier is smaller than or close to the wavelength. As the size of the barrier increases, diffraction becomes less and less pronounced. When the slit width is large enough, the diffraction pattern will no longer appear, but a bright spot produced by the light propagating in a straight line.

In this simulation we used a parallel light source instead of a laser. The main difference between a parallel light source and a laser is that the former produces a plane wave while the latter is a Gaussian beam. We have used the plane wave assumption in our theoretical derivation, so the simulation with a parallel light source can give results more similar to the theory. Further discussion of the differences between parallel light sources and lasers will be given later.

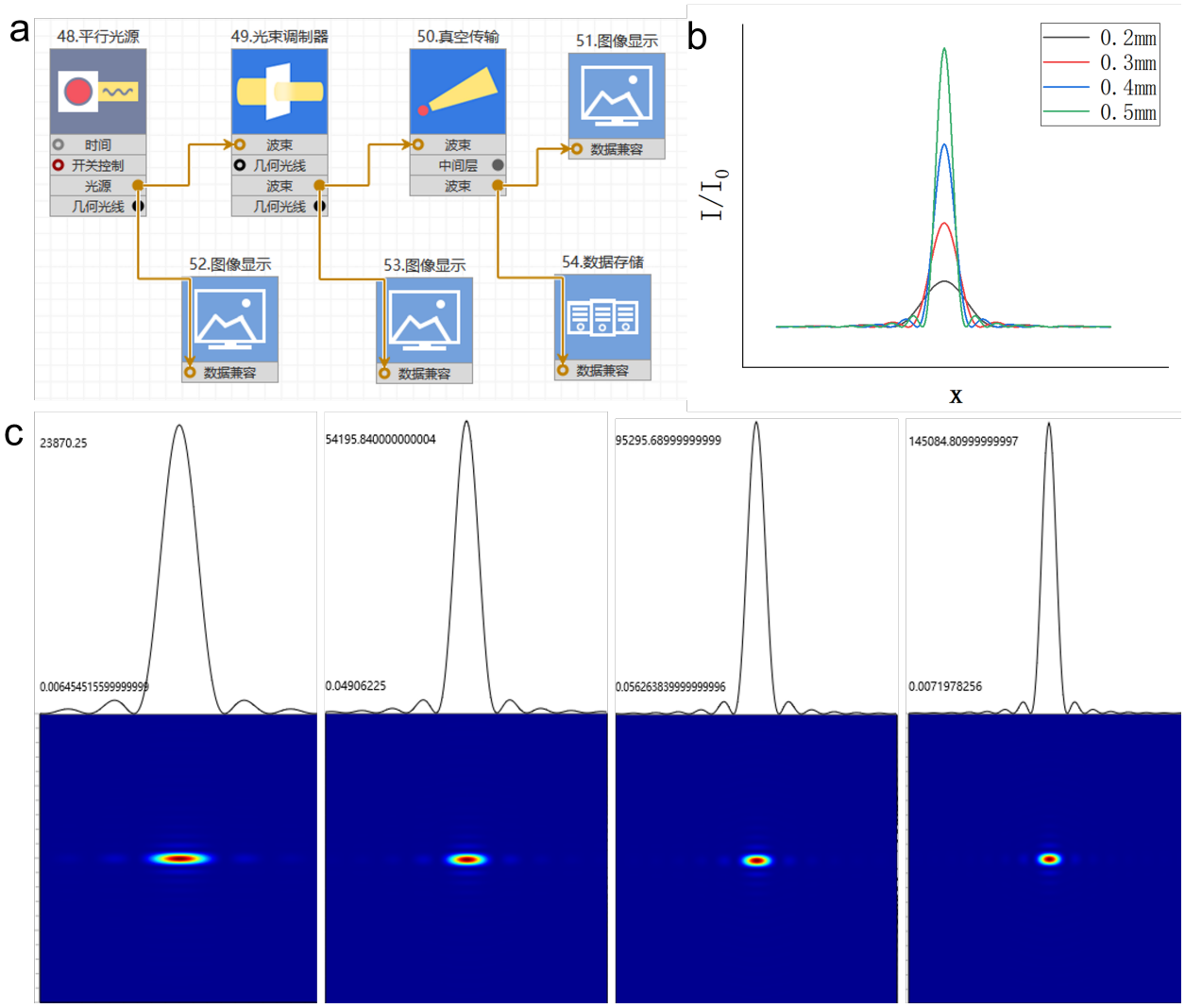

FIG. 11. (a) The device diagram of Fronhofer diffraction with a single slit. (b) The relative light intensity distribution curves of the four diffraction patterns in the same figure. (c) The diffraction patterns of these four slits with different widths.

B. Fresnel diffraction of a circular hole

We have roughly verified the correctness of the half-wave band theory of Fresnel diffraction in our experiments. In this subsection we will use simulations for a more precise verification and explore the effect of the beam expander in Fresnel diffraction.

We first performed a set of simulations without the beam expander. We set both the radius of the laser and the Gaussian beam waist to 1 mm, and the diameter of the circular hole to 0.3 mm. We theoretically calculated the positions where 2, 3, 4, and 5 half-wave bands appeared and placed the corresponding observation screens to obtain diffraction patterns, as shown in Fig.12. At the position of 2 and 4 half-wave bands, the center of the pattern is dark spot, and at the position of 3 and 5 half-wave bands, the center of the pattern is bright spot, which is in good accordance with the theory of half-wave bands.

Then we performed a set of simulations using a beam expander lens. The expanded beam mirror is a combination of a concave lens and a convex lens. We set the focal length of the concave lens to -2mm, the distance of the vacuum transmission to 3mm, and the focal length of the convex lens to 6mm, and these form a beam expander. We theoretically calculated the positions where 2, 3, 4, and 5 half-wave bands appeared and placed the corresponding observation screens to obtain diffraction patterns, as shown in Fig.13.

Comparing Fig.12 and Fig.13, we can find that the diffraction pattern with the beam expander is more blurred. We believe that this is because the beam in the beam expander is not received in its entirety, which leads to a decrease in the dimensionality in the later calculation.

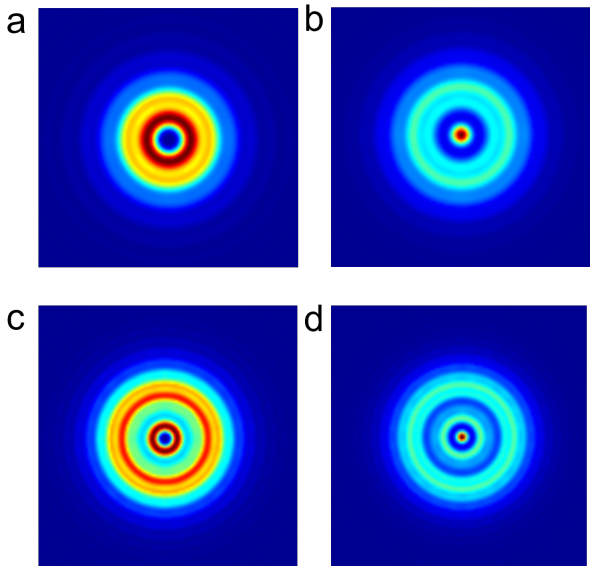

FIG. 12. Fresnel diffraction without beam expander.
(a) $\phi = 0.3$ mm, $k = 2$. (b) $\phi = 0.3$ mm, $k = 3$.
(c) $\phi = 0.3$ mm, $k = 4$. (d) $\phi = 0.3$ mm, $k = 5$.

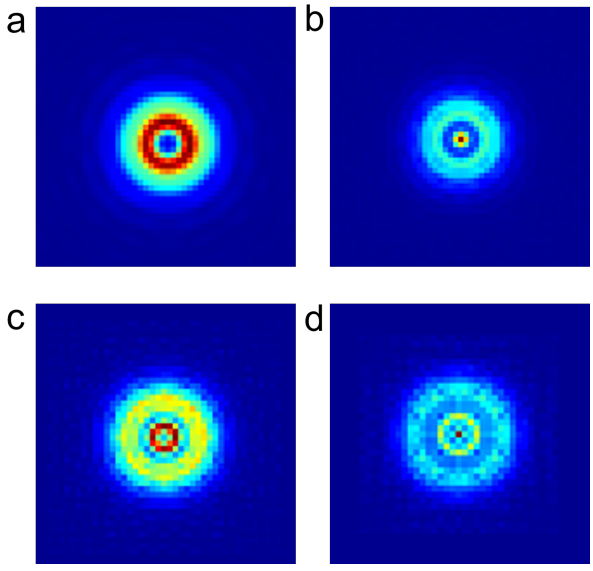

FIG. 13. Fresnel diffraction with beam expander.
(a) $\phi = 0.3$ mm, $k = 2$. (b) $\phi = 0.3$ mm, $k = 3$.
(c) $\phi = 0.3$ mm, $k = 4$. (d) $\phi = 0.3$ mm, $k = 5$.

C. The difference between laser and parallel light sources

As mentioned before, we used the assumption of plane waves in the theoretical derivation. But in reality, the laser we usually use emits a Gaussian beam. Each time the laser is reflected in the resonant cavity, it is equivalent to a diffraction occurring. Diffraction is equivalent to a Fourier transform of the wavefront.

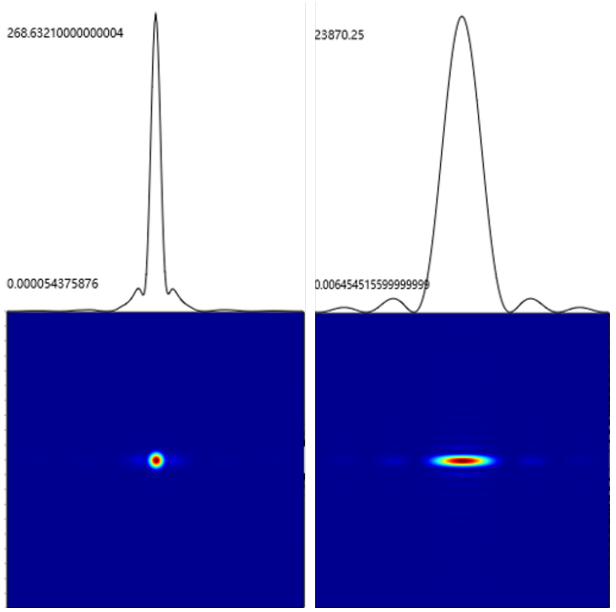

FIG. 14. Fronhofer diffraction pattern of laser and parallel light sources, when other conditions are the same. On the left is the laser, and the diffraction pattern has a clear triple split. On the right is the parallel light, and the diffraction pattern is normal.

When the wavefront amplitude distribution is a Gaussian function, the Fourier transform of the Gaussian function is still itsdelf and the wavefront distribution reaches stability. Therefore the beam from the laser is Gaussian distributed along the transverse direction.

In terms of diffraction effects, Gaussian beams differ from parallel light by three factors: the spherical wavefront, the Gaussian-type distribution of amplitudes in the beam cross-section, and the finite beam aperture.

In the literature[2] [3], the phenomenon of the triple splitting of the primary maximum in the Fronhofer diffraction of a thin filament under a Gaussian beam was proposed and explained. In the theory of the literature [3], the triple splitting of the primary maximum appears in the diffraction pattern of a fine filament under Gaussian beam irradiation, but not in the diffraction pattern of a single slit.

However, in our simulation, we observe that the triple splitting of the primary maximum also appears in the Fronhofer diffraction pattern of the single slit. [See Fig.14.]

We are not yet able to give a valid explanation. This is a problem that deserves our further study.

V. CONCLUSION

We experimentally measured the relative light intensity distribution of the pattern of Fraunhofer diffraction with a single slit, verified the formula of Fraunhofer diffraction with a single slit, and then further studied the effect of the slit width on the diffraction pattern by simulation.

Our measurements and simulations of the light field distributions in the x- and y-axis directions for Fresnel diffraction of a circular hole verify the correctness of the half-wave band theory. In addition we discuss the effect of the beam expander on Fresnel diffraction.

We have verified the Fronhofer diffraction of a circular hole by measuring the diameter of the Airy spot.

During the simulation, we found the phenomenon of the triple splitting of the primary maximum in the Fronhofer diffraction of a single slit under a Gaussian beam, and we are ready to carry out further studies.

ACKNOWLEDGMENTS

We wish to acknowledge the experimental guidance from Mrs. Zhao, and useful discussions from Tang Bei, Peng Jiahua and Wu Jinqi. In addition, we are particularly grateful to APS for the revtex series of latex templates which allow us to write this article easily and beautifully.

Finally, we **thank** seelight for simulation support.

[1] Y. Daoyin and T. hengying, *Fundamentals of Optical Engineering Tutorial* (Fundamentals of Optical Engineering Tutorial, 2007).

[2] B. G. Zhu Bing, Xiao Xudong, Fronhofer diffraction of fine filaments during gaussian beam illumination, Chinese Journal of Quantum Electronics , 130 (1988).

[3] B. G. Ye Qingwei, Fraunhofer diffraction of gaussian beam through a filament, Journal of Ningbo University , 6 (1992).

APPENDIX: Raw data of experiment

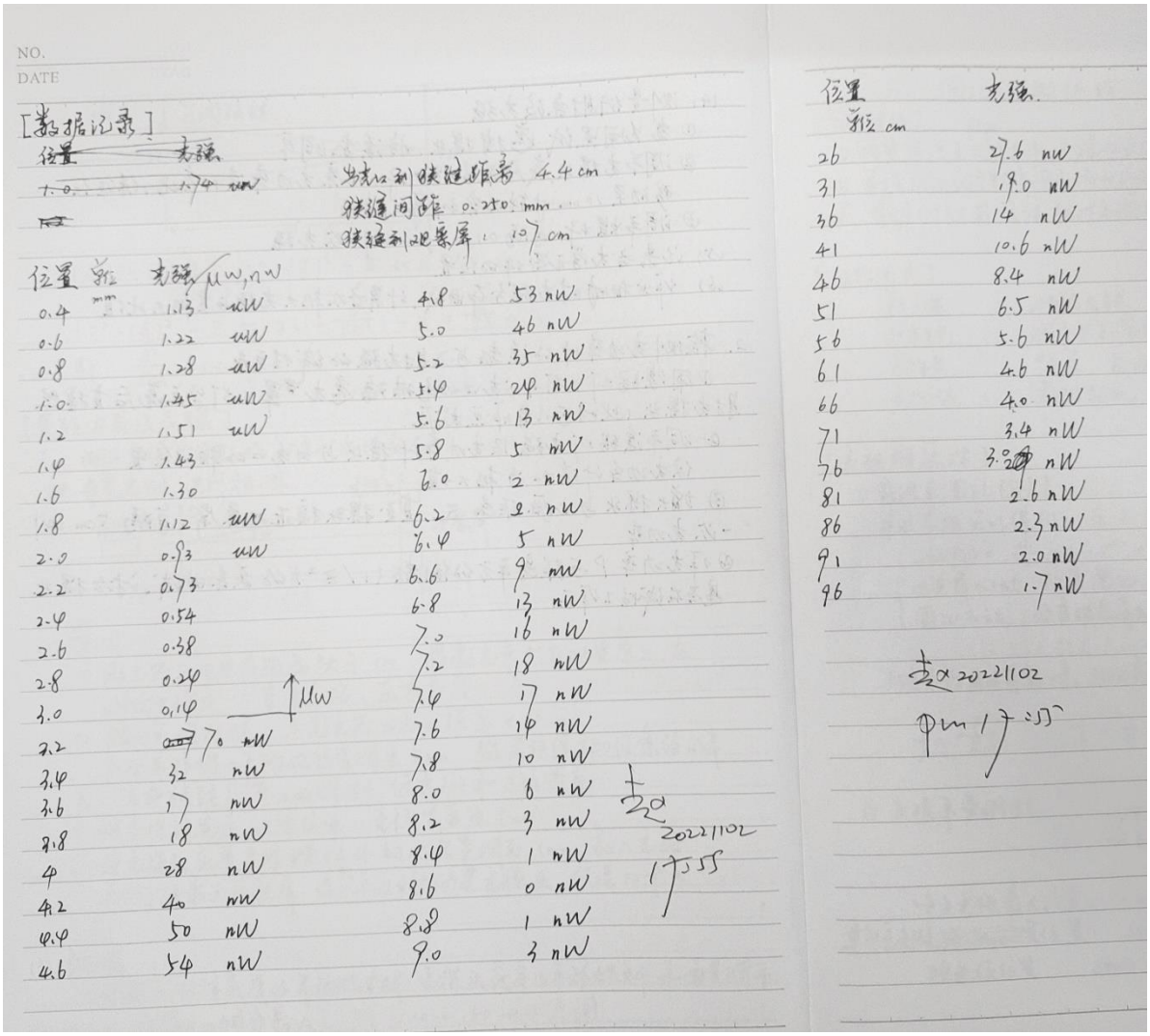

NO.
DATE

[数据记录]

~~位置 光强~~
~~1.0 1.14 uW~~

为光纤到狭缝距离 4.4 cm
狭缝间距 0.210 mm
狭缝到观察屏: 107 cm

位置 mm	光强 μW,nW
0.4	1.13 uW
0.6	1.22 uW
0.8	1.28 uW
1.0	1.45 uW
1.2	1.51 uW
1.4	1.43
1.6	1.30
1.8	1.12 uW
2.0	0.83 uW
2.2	0.73
2.4	0.54
2.6	0.38
2.8	0.24
3.0	0.14
3.2	~~700~~ 70 nW
3.4	32 nW
3.6	17 nW
3.8	18 nW
4	28 nW
4.2	40 nW
4.4	50 nW
4.6	54 nW
4.8	53 nW
5.0	46 nW
5.2	35 nW
5.4	24 nW
5.6	13 nW
5.8	5 nW
6.0	2 nW
6.2	2 nW
6.4	5 nW
6.6	9 nW
6.8	13 nW
7.0	16 nW
7.2	18 nW
7.4	17 nW
7.6	14 nW
7.8	10 nW
8.0	6 nW
8.2	3 nW
8.4	1 nW
8.6	0 nW
8.8	1 nW
9.0	3 nW

μW

王a 20221102 17:55

位置 mm	光强
26	2.6 nW
31	1.8.0 nW
36	14 nW
41	10.6 nW
46	8.4 nW
51	6.5 nW
56	5.6 nW
61	4.6 nW
66	4.0 nW
71	3.4 nW
76	3.0 nW
81	2.6 nW
86	2.3 nW
91	2.0 nW
96	1.7 nW

王a 20221102
17:55

NO.
DATE

[数据记录]

菲涅耳圆孔衍射

$f=0.75$ mm　　扩束镜 $f=4.5$ mm　　$r=0.2$ m

条纹	暗	亮	暗	亮	
位置	61.7	38.4	25.4	20.7	cm

$f=0.5$ mm

条纹	亮	暗	
位置	41.9	21.8	cm

$f=0.35$ mm

条纹	暗	亮	
位置	20.1	7.5	cm

夫琅禾费圆孔衍射

观察屏到小孔距离：1 m　　$\lambda=632.8$ nm

小孔直径 /mm	艾里斑直径 /mm
0.15	7.8
0.3	6.3
0.5	3.4

2022/11/09

19=10